Φ_s = Thiele modulus, defined by Equation (10)
ξ = R/R_o

Subscripts and Superscripts

— = average value
b = average bed condition (for particles)
c = catalyst or center
a,i = macro- and micropores, respectively
exp = experimental
g = bulk gas phase
p = pellet
s = solid or outer surface of pellet
pr = predicted
w = reactor wall condition

LITERATURE CITED

1. Carberry, J. J., *A.I.Ch.E. J.*, 7, 350 (1961).
2. Tinkler, J. D., and A. B. Metzner, *Ind. Eng. Chem.*, 53, 663 (1961)
3. Weisz, P. B., and J. S. Hicks, *Chem. Eng. Sci.*, 17, 265 (1962).
4. Satterfield, C. N., and T. K. Sherwood, "The Role of Diffusion in Catalysis," Chap. 3, Addison-Wesley, Reading, Mass. (1963).
5. Sehr, R. A., *Chem. Eng. Sci.*, 9, 145 (1958).
6. Masamune, Shinobu, and J. M. Smith, *J. Chem. Eng. Data*, 8, 55 (1963).
7. Cunningham, R. E., J. J. Carberry, and J. M. Smith, *A.I.Ch.E. J.*, 11, 636 (1965).
8. Miller, D. N., and H. A. Deans, paper presented A.I.Ch.E. San Francisco meeting (May, 1965).
9. Otani, Seiya, Noriaki Wakao, and J. M. Smith, *A.I.Ch.E. J.*, 11, 439 (1965).
10. Hutchings, John, and J. J. Carberry, *ibid.*, 12, 20 (1966).
11. Wakao, Noriaki, and J. M. Smith, *Chem. Eng. Sci.*, 17, 825 (1962).

Manuscript received December 6, 1965; revision received March 4, 1966; paper accepted March 7, 1966.

Shape of Liquid Drops Moving in Liquid Media

R. M. WELLEK, A. K. AGRAWAL

University of Missouri, Rolla, Missouri

and A. H. P. SKELLAND

University of Notre Dame, Notre Dame, Indiana

An investigation of the effects of various physical properties, drop size, and drop velocity on drop shape was carried out for nonoscillating liquid drops falling through stationary liquid continuous phases. The data of forty-five dispersed-continuous phase systems were studied with continuous phase viscosities varying from 0.3 to 46 centipoise and interfacial tensions varying from 0.3 to 42 dyne/cm. A theoretical relation was obtained from the Taylor and Acrivos analysis which quite accurately predicts drop eccentricities for drop Reynolds numbers less than about 20, but is highly inaccurate at higher Reynolds numbers. Relatively simple empirical relations involving the Weber number, Eötvös number, and viscosity ratio were obtained which enable the prediction of the eccentricity of nonoscillating drops over a wide range of Reynolds numbers (6.0 to 1,354) with average deviations of 6 to 8%. These relations may be useful in the estimation of the interfacial area, velocity, and continuous phase mass transfer coefficient of drops distorted from spherical shape.

In liquid-liquid extraction, mass transfer between phases is often facilitated by dispersing one phase in the other. Many investigators have studied mass transfer from single liquid droplets in order to obtain information which might ultimately aid in the design of large-scale extraction columns without the need for experimentally measured overall extractor efficiencies (*11, 18, 23, 26, 33, 36, 38*). Most of these studies have been based on the assumption of spherical droplets. At low droplet Reynolds numbers, droplet shape will approximate a sphere; however, at high Reynolds numbers droplets will be distorted from spherical shape. The change in shape affects not only interfacial area but also, as indicated by recent experimental and theoretical studies (*2, 24, 32*), the continuous phase mass transfer coefficient. While several investigators (*4, 6, 10, 14, 19, 22*) have reported quantitative information on the shape of liquid droplets for individual systems, currently there is no accurate means of predicting droplet shape without recourse to experiment.

It is the purpose of the present investigation to obtain a relation which will predict the shape of nonoscillating liquid droplets moving in liquid media from a knowledge of the physical properties of the Newtonian dispersed and continuous liquid phases, the droplet size, and relative droplet velocity.

PREVIOUS WORK AND THEORETICAL CONSIDERATIONS

Droplet Shape

The shape of a drop moving in a liquid continuous phase is determined by the forces acting along the surface of the drop. Basically the shape is dependent upon

the balance between the fluid dynamic pressure exerted, because of the relative velocity of the drop and continuous fluid and the interfacial forces which tend to make the drop a sphere (*13, 20*). Drops with small Reynolds numbers (either because of high μ_c or small size) are usually spherical. At high Reynolds numbers, the inertial forces tend to cause a distortion from the spherical shape. As the Reynolds number is increased, droplet oscillation (unsteady state distortion in shape) will set in; ultimately as N_{Re} increases for the above physical system, drop breakup will occur. Only nonoscillating drops will be considered in the present work.

The phenomenon of drop distortion has been classified by Kintner (*20*) according to the viscosity of the continuous phase liquid: low μ_c, Newtonian; high μ_c, Newtonian; and high $(\mu_a)_c$, non-Newtonian.

Drops moving in low viscosity liquids are first distorted to approximately an oblate spheroidal shape. As the drop size increases, the eccentricity ($E = D_H/D_V$) of the drop increases. The surface area of an oblate spheroid is given by

$$A_{os} = \frac{\pi}{2} D_H^2 + \frac{D_H D_V}{\sqrt{E^2-1}} \ln\left(E + \sqrt{E^2-1}\right) \quad (1)$$

The ratio of the area of an oblate spheroid to that of a sphere of equal volume is (*10*):

$$\frac{A_{os}}{A_s} = \frac{1}{2} E^{2/3} + \frac{1}{E^{1/3}\sqrt{E^2-1}} \left[\ln\left(E + \sqrt{E^2-1}\right)\right] \quad (2)$$

At eccentricities of 1.5, 2, 2.5, and 3, the above ratio is approximately 1.031, 1.095, 1.17, and 1.26, respectively.

As the drop equivalent diameter corresponding to the maximum (or first point of inflection) of the terminal velocity-drop diameter curve (near the onset of oscillation) is approached, horizontal planar symmetry is lost, that is, the front of the drop becomes more flattened than the rear (*7, 20*) (see Figure 1). The eccentricity of a drop is often reported without any quantitative indication of flattening ($D_{v,u}/D_{v,l}$).

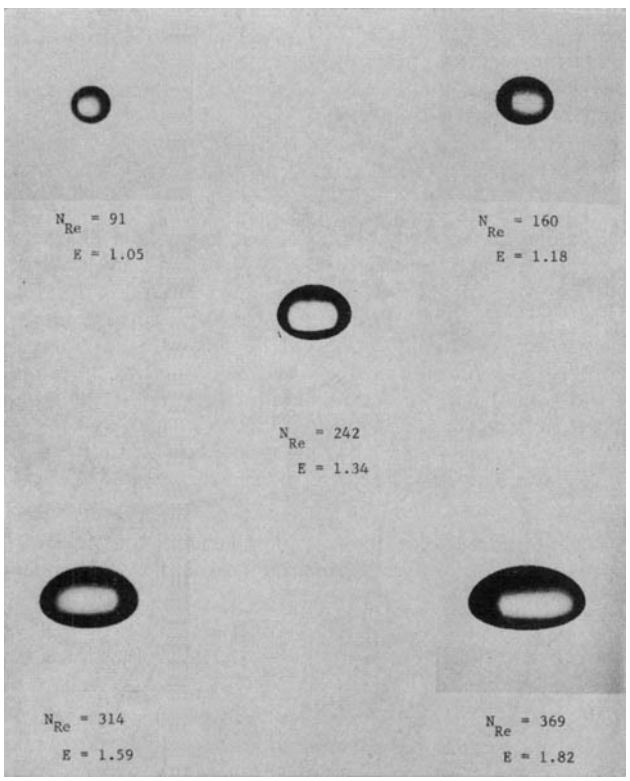

Fig. 1. Photographs of moving droplets; glyceryl triacetate and water (system 27).

Eccentricity data are usually presented as a plot of E vs. D_e (see Figures 3, 4, and 5). Several investigators (*10, 19, 22*) have reported essentially linear relationships for a particular liquid-liquid system. However, the eccentricity-drop size relation was reported to be nonlinear for the smallest drop sizes (*22*). Some of these data have included average eccentricities for oscillating drops.

With regard to the effect of physical properties, Keith and Hixson (*19*) indicate that

$$E \propto \sigma^{-1.0}\, \Delta\rho^{1.0} \quad (3)$$

whereas Klee and Treybal (*22*) indicate that

$$E \propto \sigma^{-1.0}\, \Delta\rho^{1/2} \quad (4)$$

and Garner and Tayeban (*10*) indicate that perhaps

$$E \propto \mu_d^{-m} \quad m = \text{positive number} \quad (5)$$

although they do not give any value for m.

Several authors have attempted to predict droplet eccentricity by theoretical or semitheoretical relations.

Saito (*31*) extended the work of Rybczynski (*30*) on the motion of a viscous spherical drop through a viscous fluid in the low Reynolds number region by taking into account the second-order velocity terms in the equation of motion. A relation is given which may be used to predict whether a droplet will be either a prolate or oblate spheroid.

$$\Delta = \frac{\rho_d}{3}\left(1 + \frac{\mu_d}{\mu_c}\right) - \rho_c\left[\frac{10}{3} + \frac{319}{30}\left(\frac{\mu_d}{\mu_c}\right) + \frac{37}{5}\left(\frac{\mu_d}{\mu_c}\right)^2 + \frac{1}{20}\left(\frac{\mu_d}{\mu_c}\right)^3\right] \quad (6)$$

If $\Delta > 0$, the distortion is prolate; if $\Delta < 0$, the distortion is oblate. Prolate distortion, as given by Equations (6) and (7), basically is a result of high-density ratios or low-viscosity ratios. Taylor and Acrivos (35), in a theoretical study of drop deformation at low Reynolds number [< 0 (1)], corrected an error in the work of Saito. Their expression for Δ is as follows

$$\Delta = \left(\frac{\rho_d/\rho_c - 1}{12}\right)\left(1 + \frac{\mu_d}{\mu_c}\right) - \left[\frac{81}{80}\left(\frac{\mu_d}{\mu_c}\right)^3 + \frac{57}{20}\left(\frac{\mu_d}{\mu_c}\right)^2 + \frac{103}{40}\left(\frac{\mu_d}{\mu_c}\right) + \frac{3}{4}\right] \quad (7)$$

which qualitatively agrees with the previous work of Saito. The use of the work of Saito and Taylor and Acrivos to predict droplet eccentricity will be examined in a later section.

Hughes and Gilliland (*16*) have proposed a method of predicting the eccentricity of drops in the range of intermediate and high Reynolds numbers. The development is based on the suggestion of Spilhaus (*34*) that the force tending to separate the drop laterally can be considered as proportional to the area over which it acts and to the kinetic head $\rho_c U^2/2$ of the continuous phase. The dimensionless proportionality factor, termed the *distortion coefficient* (γ), is similar to the drag coefficient. They obtained the relation

$$\frac{1}{4}\gamma\frac{N_{Re}^2}{N_{Su}} = \psi(h) \quad (8)$$

where the function $\psi(h)$ is presented in Table 1 of reference *16*. This relation may also be expressed as

$$\frac{1}{4}\gamma N_{We} = \psi\left(\frac{1}{E}\right) \tag{9}$$

Using eccentricity data for gaseous continuous systems, Hughes and Gilliland calculated values of γ. These values were empirically correlated by the following expression:

$$\gamma = 0.0102\,[N'_{Re}]^{0.35} = 0.0102\,[N_{Re}\,E^{1/3}]^{0.35} \tag{10}$$

The method was not recommended for application to liquid continuous phase systems. Klee and Treybal (*22*) were unsuccessful in their attempt to correlate their data for liquid continuous phases through the use of the distortion coefficient, γ.

Harmathy (*13*) has attempted to describe the shape of fluid particles by means of a force balance at the particle interface. However, rather than solve the force balance relation for the particle shape, he suggested that the unknown relation be left as

$$\text{shape} = f_1\left[\frac{D_e U^2 \rho_c}{\sigma}, \frac{g\Delta\rho D_e^2}{\sigma}\right] = f_1[N_{We}, N_{Eo}] \tag{11}$$

The shape is, of course, a function of the eccentricity E.

The effect of a finite viscosity of the fluid particles μ_d was neglected in the above analysis; hence, it is expected that the effect on droplet shape of circulation within the drop was neglected. Harmathy was interested only in the high N_{Re} (> 500), and in this turbulent region, N_{Eo} is directly proportional to N_{We}. Therefore

$$E = f_2\,(N_{Eo}) \qquad N_{Re} > 500 \tag{12}$$

A plot of E vs. N_{Eo} for air bubbles in various liquids, water drops in air, and liquid drops in liquid media indicated considerable scatter (see Figure 2, reference *13*). One reason for this scatter may be droplet oscillation, which in the case of liquid-liquid systems usually occurs for Reynolds numbers greater than 500. The solid curve on this plot was obtained by Harmathy, who used his semiempirical drag coefficient — N_{Eo} graphical relation for fluid particles and an approximate relation of Riabouchinsky (*29*) for the effect of eccentricity on the drag coefficient of an oblate spheroid. For liquid droplets in the turbulent flow regions ($0.7 \lessapprox N_{Eo} \lessapprox 14$), this relation can be expressed by the following implicit function by using an approximation given by Harmathy:

$$1.12\,N_{Eo}^{1/2} = E^{2/3}\,(2.5 - 1.5/E) \quad N_{Re} > 500 \tag{13}$$

Elzinga and Banchero (*4*) have suggested that the assumption that internal circulation has little effect on distortion probably holds for most systems where drops are dispersed in a gas, but the assumption is probably not good for a liquid continuous phase. They also point out that surface-active agents have an important effect on distortion. In their system, surface-active agents decreased droplet distortion, while the static interfacial tension, viscosities, and densities did not reflect the presence of these agents. Garner and Skelland (*9*) have observed a similar effect of contaminants on droplet shape.

In a recent study of the shape of nonoscillating liquid drops falling in gases, Reinhart (*28*) obtained the following relation:

$$E = 1.0 + 0.130\,N_{Eo} \quad (1 < N_{Eo} < 8.2) \tag{14}$$

The continuous phase viscosity is very low in this case, whereas for a liquid continuous phase, μ_c would be expected to have a significant effect on droplet shape. Garner and Lihou (*39*) have presented complex relations for the shape of gas bubbles rising in liquid media which employ dimensionless groups in a manner similar to that used by Hu and Kintner (*15*) for predicting terminal velocities of liquid drops. This method considers both symmetric and nonsymmetric oblate spheroidal shapes.

Nonoscillating droplet shapes other than spheres and oblate spheroids have been observed when a liquid drop moves through a high-viscosity liquid phase (*5, 7, 8, 20, 25, 37*). Fararoui and Kintner (*5*) report the appearance of a prolate shape drop if a drop of low-viscosity liquid moves through corn syrup of viscosity about 300 centipoise. As drop size is increased the shape is progressively spherical, prolate spheroidal, spherical, oblate spheroidal, nonsymmetrical spheroidal, and ultimately an inverted mushroomlike shape with an indented rear surface. Equation (*6*) has predicted the appearance of prolate droplets (*16, 20*). When large drops move through non-Newtonian liquid media of high apparent viscosities, the same shapes as for high μ_c Newtonian fluids have been observed; however, for some drop sizes, the classical teardrop shape with trailing filament has been observed.

Almost all the eccentricity data reported in the literature are for systems in which organic liquid drops fall (or rise) in an aqueous continuous phase ($\mu_c \approx 1.0$ centipoise). Thus the effect of low μ_c (< 0.8 centipoise) or moderately high μ_c (1.2 to 50 centipoise) on drop shape cannot be quantitatively predicted. Since the Harmathy (*13*) relation for drop eccentricity was developed with oscillating drop data, there is currently no relationship for accurately predicting the eccentricity of nonoscillating droplets over a wide range of Reynolds numbers.

Effect of Droplet Shape on Mass Transfer

Mass transfer studies described below for solid-gas and gas-liquid dispersed and continuous phase systems indicate that the shape of the dispersed phase affects not only the interfacial area and velocity but also the rate of mass transfer. It is possible that similar effects occur in liquid-liquid systems.

Skelland and Cornish (*32*) were able to correlate the mass transfer rates of sublimation of oblate napthalene spheroids in an air stream by using a j factor–Reynolds number type of correlation.

$$j_D = \frac{N'_{Sh}}{N''_{Re}\,(N_{Sc})^{1/3}} = 0.74\,(N''_{Re})^{-0.50} \tag{15}$$

The above correlation was obtained by using a characteristic dimension D_3 proposed by Pasternak and Gauvin (*27*) in the Sherwood number and Reynolds number, rather than D_e. This dimension—the total surface area of the particle (an oblate spheroid in this case) divided by the perimeter normal to flow—can be shown to be related to the eccentricity and equivalent diameter of the spheroid as follows:

$$D_3 = \frac{\pi}{2}\left[E^{1/3} + \frac{\ln\,(E + \sqrt{E^2 - 1})}{E^{2/3}\sqrt{E^2 - 1}}\right] D_e \tag{16}$$

Lochiel and Calderbank (*24*) derived the following expression from the experimental correlation of Skelland and Cornish (*32*):

$$\gamma_1 = \frac{(k_c)_{os}}{(k_c)_s} = \left[\frac{A_s}{A_{os}}\right]^{1/2} E^{1/6} \tag{17}$$

which compared very favorably with their theoretically derived expression based upon boundary-layer flow analysis for oblate spheroids with immobile interfaces. For oblate spheroids with mobile interfaces the following relation was derived (*24*):

$$\gamma_2 = \frac{(k_c)_{os}}{(k_c)_s} = \frac{A_s}{A_{os}} [2/3\ (1 + k)] \qquad (18a)$$

where

$$k = -\frac{eE^2 - E \sin^{-1} e}{e - E \sin^{-1} e} \qquad (18b)$$

$$e = \left[1 - \frac{1}{E^2}\right]^{1/2} \qquad (18c)$$

$$\frac{(k_c)_s D_e}{D} = 1.13 \left[\frac{D_e U}{D}\right]^{1/2} \qquad (19)$$

γ_1 and γ_2 are plotted as functions of E in Figures 2 and 4, respectively, in reference 24.

Calderbank and Lochiel (2) have applied Equations (18) and (19) in studies of the dissolution of single bubbles of carbon dioxide rising in water.

EXPERIMENTAL

The object of the experiments was to measure the deformation (eccentricity) of a single stream of nonoscillating drops falling (or rising) in a stationary liquid continuous phase.

Systems

Twenty-eight dispersed phase-continuous phase systems were experimentally investigated in this work. In addition to the above systems, the eccentricity data of seventeen other systems were obtained from the literature.

All organic liquids were purified by batch distillation except for ethylene glycol and corn oil; laboratory distilled water was used in all experiments. All systems were mutually saturated before the eccentricity and physical property measurements except the water-corn oil system (essentially immiscible) and systems 23, 25, and 27 (see Table 1). Systems 23, 25, and 27 were used to study the effect of mass transfer on shape. The effect of mass transfer was not negligible in system 25. In five systems both directions of dispersion were used for

TABLE 1. PHYSICAL PROPERTIES

Liquid-liquid system*	σ, dyne/cm.	μ_c centipoise	μ_d centipoise	ρ_c g./cc.	ρ_d g./cc.	T, °C.	Source
1. Ethylene glycol and benzene	7.4	0.57	12.21	0.8689	1.0936	27.0	This work
2. Water and corn oil	23.4	45.93	0.86	0.9135	0.9997	28.0	This work
3. Ethylene glycol and hexane	14.2	0.31	14.56	0.6657	1.1057	26.7	This work
4. Nitrobenzene and ethylene glycol	4.9	13.55	1.78	1.1134	1.1952	26.7	This work
5. Aniline and water	6.6	0.86	3.08	0.9973	1.0157	27.2	This work
6. Bromobenzene and water	34.2	0.83	0.73	0.9967	1.0985	27.0	This work
7. Water and hexane	32.1	0.32	0.84	0.6655	0.9961	26.7	This work
8. Water and MIBK	9.7	0.55	0.87	0.7985	0.9941	27.2	This work
9. Water and MIBK	10.4	0.54	0.81	0.7956	0.9958	29.3	This work
10. Carbon tetrachloride and water	31.1	0.85	0.89	0.9964	1.5782	28.9	This work
11. Nitrobenzene and water	13.5	0.85	1.71	0.9973	1.1963	27.0	This work
12. Nitrobenzene and water	22.1	0.88	1.78	0.9968	1.1974	24.9	This work
13. Water and ethylbenzene	35.0	0.62	0.87	0.860	0.9965	26.0	This work
14. Ethylbenzene and water	34.9	0.87	0.62	0.9965	0.860	26.0	This work
15. Chlorobenzene and water	35.0	0.86	0.74	0.9965	1.0989	27.0	This work
16. Water and chlorobenzene	34.0	0.72	0.80	1.0960	0.9957	30.0	This work
17. Water and nitrobenzene	22.7	1.80	0.89	1.1980	0.9971	25.0	This work
18. Benzaldehyde and water	14.38	0.85	1.33	0.9965	1.0380	27.3	This work
19. Water and benzaldehyde	14.16	1.29	0.82	1.0365	0.9960	29.0	This work
20. MIBK and water	10.2	0.89	0.58	0.9969	0.8011	25.5	This work
21. Benzyl alcohol and water	3.6	0.85	4.76	0.9965	1.0398	27.3	This work
22. Water and benzyl alcohol	3.6	4.76	0.85	1.0398	0.9965	27.3	This work
23. Glycol diacetate and water†	2.3	0.92	2.62	0.9971	1.0990	24.2	This work
24. Glycol diacetate and water	2.3	1.35	2.44	1.0226	1.0976	24.2	This work
25. Ethyl acetoacetate and water†	3.5	0.895	1.50	0.9970	1.0194	25.0	This work
26. Ethyl acetoacetate and water	3.5	1.13	1.58	1.0054	1.0220	25.0	This work
27. Glyceryl triacetate and water†	4.0	0.91	16.6	0.9971	1.1531	24.7	This work
28. Glyceryl triacetate and water	4.0	0.94	10.9	1.0002	1.1472	24.7	This work
29. Methyl ethyl ketone and water	0.3	1.45	0.60	0.9600	0.8370	23.0	22
30. Sec-butyl alcohol and water	0.6	1.56	2.78	0.9705	0.8660	24.5	22
31. Nonyl alcohol and water	4.9	1.00	16.2	0.9982	0.8242	20.0	22
32. Methyl butyl ketone and water	9.8	0.93	0.60	0.9947	0.8155	26.0	22
33. Oil (S.A.E. 10W) and water	18.5	1.06	0.721	0.9975	0.8650	26.5	22
34. Benzene and water	30.0	1.14	0.68	0.9975	0.8870	24.0	22
35. Benzene and 20% aqueous sucrose	30.1	1.39	0.59	1.0600	0.8720	23.0	22
36. Kerosene and water	40.4	1.08	1.47	0.9986	0.8071	28.0	22
37. Pentachloroethane and water	42.4	0.95	2.03	0.9978	1.6740	18.0	22
38. 2. Ethyl-hexane 1.3 diol and water	4.0	1.0	85.0	0.998	0.945	20.0	10
39. Benzyl alcohol and water	5.0	1.0	5.3	0.998	1.0420	20.0	10
40. *n*-Butyl alcohol and water	1.8	1.19	2.74	0.9865	0.8427	—	19
41. Ethyl acetate and water	4.5	1.20	0.48	0.9922	0.8988	—	19
42. MIBK and water	10.7	0.93	0.58	0.9950	0.8006	—	19
43. *n*-Butyl chloride and water	24.2	0.92	0.43	0.9957	0.8784	—	19
44. Toluene and water	35.6	0.89	0.55	0.9969	0.8606	—	19
45. Cyclohexane and water	40.7	0.90	0.88	0.9968	0.7723	—	19

* Dispersed phase mentioned first.

† Phases not mutually saturated.

a range of drop sizes (that is, phase A dispersed in B, then phase B dispersed in A). Densities were measured with pycnometers, viscosities with a U-tube viscometer, and interfacial tensions with ring tensiometer. These physical properties appear in Table 1 (systems 1 through 28) at the temperature of the eccentricity experiments. Two liquid-liquid systems were studied at two different temperatures (systems 8, 9, 11, and 12). The reported physical properties of the systems studied in the literature are also presented in Table 1 (systems 29 to 45).

Equipment

The dispersed phase was stored in a 50-cc. constant-head buret fitted at the bottom with a Teflon needle valve. The needle valve is designed for use with a wide range of nozzle sizes, thus enabling the formation of different drop sizes. Large nozzles were made of thin-walled glass tubing with the tip ground so that the plane of the tip was at right angles to the axis of the nozzle. The smaller nozzles were stainless steel hypodermic needles with the tips ground to a sharp conical edge.

The continuous phase was contained in a 7.6-cm. I.D. glass column, 92 cm. high. The bottom of the column was sealed by a stainless steel plate connected to the column by a flange with a Teflon gasket. The droplets were photographed during free fall (or rise) through a custom-made central viewing section of optically plane glass to eliminate optical distortion effects of the cylindrical column (see Figure 2). If the dispersed phase was heavier than the continuous phase, the nozzles were attached directly to the buret needle valve, and the buret-nozzle assembly was lowered so that the nozzle tip was just below the surface of the continuous phase. If the dispersed phase was lighter than the continuous phase, the nozzles were attached to a special fitting on the bottom plate; the dispersed phase was fed from the buret to the nozzles by means of Teflon tubing.

Procedure

Droplets were formed at a frequency of about 12 drops/min. The number of droplets formed during each run was recorded along with the total volume of dispersed phase which passed through the column; this enabled the average drop volume in a given run to be calculated. Droplet fall velocities were obtained with a stopwatch accurate to $\pm$ 0.05 sec. for a free fall (or rise) distance of approximately 50 cm.; the average of about fifteen measurements for each run was recorded.*

The photographic techniques employed are similar to those reported in the literature (*21*). For systems 9 and 12 through 28, a 4 $\times$ 5 Speed Graphic Camera with a Kodak Ektar f 4.7, No. 2 Supermatic lens was used. The camera was mounted on one side of the droplet viewing section and was focused on a rod held in the center of the column. An electronic flash was mounted on the opposite side of the column with a light diffuser placed between the flash and the column. Kodak Contrast Process Ortho film was used, and the camera was set for time exposure. When the droplet passed the viewing section, the electronic flash ($\approx$ 1/1,000 sec.) was triggered and the droplet profile photographed. For systems 1 through 8 and 10, a Nikkorex F 35-mm. camera with 55-mm. f2 lens was used. Photo flood lamps were used for backlighting and a light diffuser was employed. Polaroid plastic sheets were placed on both sides of the viewing windows in order to obtain better droplet profiles for systems 6, 7, and 8. Kodak Tri X, 400 ASA film was used, and the camera shutter was set for a time of exposure of 1/1,000 of a sec.

Three photographs were taken of each particular droplet size, at the beginning, middle, and end of the run. Eccentricities were determined by projecting the droplet photographs onto a wall and measuring the major and minor axes. The recorded eccentricity is the average of these three photographs. Examples of the droplet profiles for the glyceryl triacetate–water system (system 27) may be seen in Figure 1. In a few systems (23 to 28), the ratio of the semiminor axes was measured to give some indication of the flattening of the droplets.*

* Tabular material has been deposited as document 8768 with the American Documentation Institute, Photoduplication Service, Library of Congress, Washington 25, D. C., and may be obtained for $1.25 for photoprints or 35-mm. microfilm.

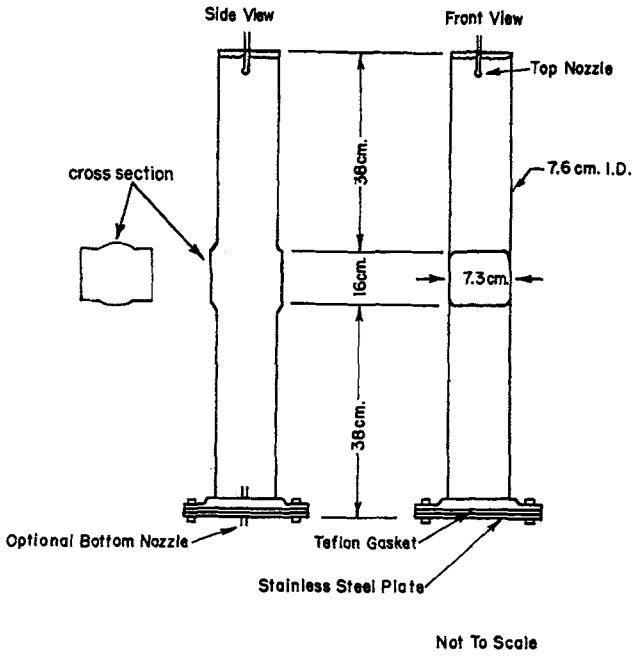

Fig. 2. Diagram of column for eccentricity experiments.

It was necessary to reject some of the eccentricity data reported in the literature, because the droplets were suspected to be oscillating. If the droplet diameter was greater than the diameter for the maximum gross terminal velocity for a system, the corresponding eccentricity data were rejected.

The original data obtained in these experiments and the literature data which were used in this work are tabulated elsewhere.*

RESULTS

The object of this investigation was to determine a functional relation between the deformation (eccentricity) of *nonoscillating* liquid droplets moving in a liquid continuous phase and such variables as droplet velocity, droplet size, and the physical properties of the system:

$$E = \psi_1 (U, \sigma, D_e, \mu_c, \mu_d, \rho_c, \Delta\rho, g) \qquad (20)$$

Proportionality relations such as Equations (3) and (4) are of use in the determination of ψ_1; however, it must be noticed that these relations have been based upon data for both oscillating and nonoscillating droplets. In this work, all analyses were restricted to a study of nonoscillating eccentricity data. It was felt that the shape of both oscillating and nonoscillating droplets probably cannot both be accurately described by the same relation, at least not a relatively simple relation.

Comparison with Previous Relations

Attempts to derive an accurate relation ψ_1 from assumed theoretical models have not been successful for liquid continuous phases (*4, 13, 16, 22*) except at very low Reynolds numbers.

The utility of the Hughes and Gilliland (*16*) relation [Equation (9)] was reexamined in this work with only nonoscillating droplet data in hopes of determining a relation for γ. The value of the distortion coefficient γ ranged from 0.081 to 1.45 with an approximate average value of 0.3. The distortion coefficient definitely does not follow the form of Equation (10) for gaseous continuous phases. No relation could be found between γ and any combination of variables.

* See footnote on this page.

The relation obtained by Harmathy (*13*) [Equation (13)] for droplets in the turbulent region ($N_{Re} > 500$) was compared with the experimental data for nonoscillating droplets, even though the Reynolds number of nonoscillation is usually less than 500. Of the nonoscillating eccentricity data studied in this investigation, about 75% had Reynolds numbers less than 500. The average absolute deviation of the data for the forty-five systems from the Harmathy relation was 16.7% for N_{Re} greater than 500, 12.6% for N_{Re} less than 500, and 13.8% for all data. One would have expected Harmathy's relation to have been more accurate in the N_{Re} range greater than 500 than in the range less than 500. It was also observed that the Harmathy relation was not very accurate for continuous phase viscosities greater than about 2 centipoise.

Theoretical Relations for $N_{Re} < 0$ (1)

In their theoretical analysis, Taylor and Acrivos (*35*) developed relations for drop deformation subject to the limitations that both $N_{Re} < 0(1)$ and $(\rho_d/\rho_c)(\mu_c/\mu_d)N_{Re} < 0(1)$. Their equation for the surface of the drop is

$$R = 1 + \zeta(\mu) \tag{21}$$

where

$$\mu = \cos\theta$$

$$\zeta = -\frac{\lambda N_{We} P_2(\mu)}{2} - \left[\frac{3\lambda\left(11\frac{\mu_d}{\mu_c} + 10\right)}{140\left(\frac{\mu_d}{\mu_c} + 1\right)}\right]\frac{N^2_{We}}{N_{Re}} P_3(\mu) \tag{22}$$

$$\lambda = \frac{1}{4\left(\frac{\mu_d}{\mu_c} + 1\right)^3}\left\{\left[\frac{81}{80}\left(\frac{\mu_d}{\mu_c}\right)^3 + \frac{57}{20}\left(\frac{\mu_d}{\mu_c}\right)^2 + \frac{103}{40}\left(\frac{\mu_d}{\mu_c}\right) + \frac{3}{4}\right] - \frac{(\rho_d/\rho_c - 1)}{12}\left(\frac{\mu_d}{\mu_c} + 1\right)\right\} \tag{23}$$

The drop eccentricity is obtained from the following relation

$$E = \frac{1 + \zeta_H}{1 + \zeta_V} \tag{24}$$

by using Equations (21), (22), and (23). This relation will be compared with experimental data later in this section.

It is of interest to consider also the theoretical expressions developed by Saito (*31*) to describe the slight deformation of drops when $N_{Re} < 0(1)$. Saito has shown that the shape of a slightly deformed drop may be represented by

$$\mathrm{r} = a + \frac{\mathrm{r}^2}{a} E_2 P_2(\cos\theta) \tag{25}$$

Table 2. The Range of Variables Studied

Variable		Range	Units
Interfacial tension	σ	0.3 to 42.4	dynes/cm.
Continuous phase viscosity	μ_c	0.3 to 45.9	centipoise
Dispersed phase viscosity	μ_d	0.5 to 85.0	centipoise
Continuous phase density	ρ_c	0.6655 to 1.1995	g./cc.
Dispersed phase density	ρ_d	0.7723 to 1.6740	g./cc.
Reynolds number	N_{Re}	6.0 to 1354	
Weber number	N_{We}	0.194 to 12.6	
Eötvös number	N_{Eo}	0.144 to 9.59	
Froude number	N_{Fr}	0.0185 to 2.26	
Viscosity ratio	$N_{\mu r}$	0.0117 to 53.4	

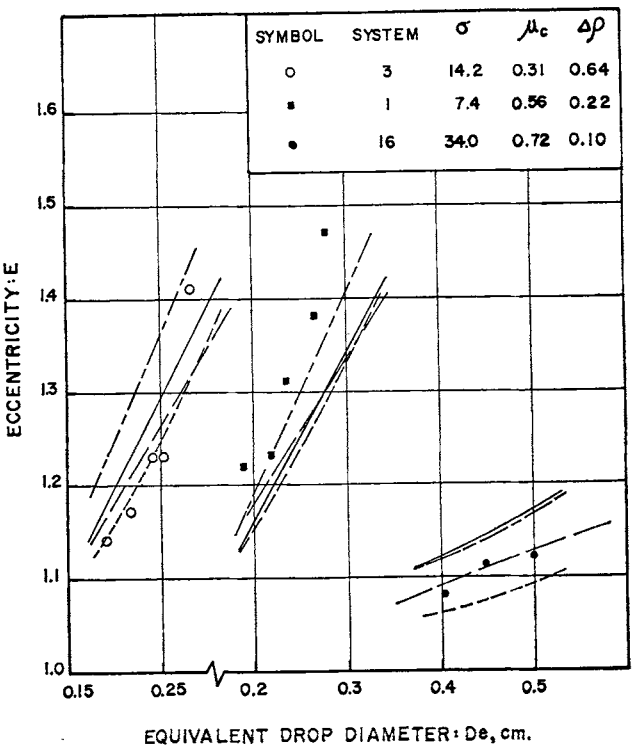

Fig. 3. Observed and calculated eccentricity as a function of drop diameter in the low μ_c region. Equation [31] — — — — —. Equation [32] ————. Equation [33] - - - - - - - - - - - - -. Equation [34]. —— —— ——.

When θ is equal to zero, $P_2(\cos\theta)$ is equal to unity; therefore, Equation (25) may be rearranged to give

$$E_2 = \frac{(\mathrm{r} - a)\,a}{\mathrm{r}^2} = \frac{(D_V - D_e)\,D_e}{D_V{}^2} = E^{2/3} - E^{4/3} \tag{26}$$

The following slightly modified relation was developed by Saito:

$$E_2 = \frac{1}{32} N_{We}\left\{\frac{\rho_d/\rho_c}{3(1 + \mu_d/\mu_c)^2} - \left[\frac{\frac{1}{20}\left(\frac{\mu_d}{\mu_c}\right)^3 + \frac{37}{5}\left(\frac{\mu_d}{\mu_c}\right)^2 + \frac{319}{30}\left(\frac{\mu_d}{\mu_c}\right) + \frac{10}{3}}{(1 + \mu_d/\mu_c)^3}\right]\right\} \tag{27}$$

Elimination of E_2 by combining Equations (26) and (27) gives a relation between the eccentricity of a drop (E) and N_{We}, (μ_c/μ_d), and ρ_d/ρ_c. According to Taylor and Acrivos (*35*), the development by Saito is in error, and Equation (27), therefore, should also be in error. Despite this error, the relation obtained by combining Equations (26) and (27) is compared with experimental data below.

The relations based on the work of Taylor and Acrivos [Equation (24)] and Saito [Equations (26) and (27)] were compared with the data for all forty-five systems (one hundred and ninety-eight eccentricity measurements). The range of variables is indicated in Tables 1 and 2. About 25% of the data was for $N_{Re} > 500$ and about 94% of the data was for $N_{Re} > 20$ (systems 2, 4, 22, 29, and 30 produced droplets with $N_{Re} < 20$). The relation based on the work of Taylor and Acrivos compared more favorably with the data than that based on the Saito development. The calculated values of eccentricity were almost always larger than the observed values

for both relations. In a comparison with *all* data, the average deviation was −92.3% for the Taylor and Acrivos relation and −3,700% for the Saito relation. Both relations were reasonably accurate even at Reynolds numbers as high as 200, provided μ_c/μ_d was greater than about 2. The average percentage deviation of the calculated eccentricity for N_{Re} less than 20 (a total of thirteen data points) was −6.1% for the Taylor and Acrivos relation and −25.6% for the Saito relation. If N_{Re} was less than 20 and μ_c/μ_d was greater than 2 (a total of eleven data points), the average percentage deviation was −5.5% for the Taylor and Acrivos relation and −8.8% for the Saito relation. Unfortunately no data were available for $N_{Re} < 0(1)$, which is the range in which both the Taylor-Acrivos and Saito relations rigorously apply. It should be recalled that the transition from streamline to eddying flow outside a drop has been observed to occur at drop Reynolds numbers of about 20 (*9, 12*); this would probably account for the poor accuracy of both relations at Reynolds numbers above 20.

Experimental Correlations

Because the functional relations for droplet eccentricity described above are restricted in use for either $N_{Re} \lessapprox 20$ or $N_{Re} \gtrapprox 500$, other relations applicable over the entire Reynolds number range were sought.

Equation (20) may be transformed by dimensional analysis into the following function:

$$E = \psi_3\left[\frac{D_e U^2 \rho_c}{\sigma}, \frac{D_e U \rho_c}{\mu_c}, \frac{g\Delta\rho D_e^2}{\sigma}, \frac{U^2}{g D_e}, \frac{\mu_c}{\mu_d}\right] \tag{29a}$$

or by identifying the dimensionless groups

$$E = \psi_3[N_{We}, N_{Re}, N_{Eo}, N_{Fr}, N_{\mu_r}] \tag{29b}$$

Only the Froude number N_{Fr} has not appeared in the previously discussed relations for predicting the eccentricity. See reference *1* for a general discussion of the physical significance of these groups.

The following functional relation was assumed to describe droplet eccentricity:

$$E - 1 = a_o N_{We}^{a1} N_{Re}^{a2} N_{Eo}^{a3} N_{Fr}^{a4} N_{\mu_r}^{a5} \tag{30}$$

A multiple regression analysis program (*3*) was used in the data analysis which progressively adds independent variables; it starts with the most important and ends when any remaining dimensional groups are statistically insignificant to the correlation. The following correlations were obtained:

$$E = 1.0 + 0.091\ N_{We}^{0.95} \tag{31}$$

$$E = 1.0 + 0.093\, N_{We}^{0.98} N_{\mu_r}^{0.07} \tag{32}$$

The average absolute deviation of the data (one hundred and ninety-eight eccentricity measurements) from these relations is 6.2 and 6.0%, respectively. The confidence limits of the exponents at the 95% probability level are:

$$0.95 \pm 0.09;\ 0.98 \pm 0.09;\ 0.07 \pm 0.04$$

These equations apply over the entire range of Reynolds numbers (6.0 to 1,354).

In view of the previous use of the Eötvös number (*13, 28*) to predict droplet eccentricity, it was surprising that the Weber number was found to be statistically more important than the Eötvös number. Therefore, the data were also correlated by using least squares methods by two relations containing *only* N_{Eo}:

$$E - 1 = b_o\ N_{Eo} \tag{33}$$

$$E - 1 = b_1\ N_{Eo}^{b2} \tag{34}$$

The coefficients b_o, b_1, and b_2 are 0.129, 0.163, and 0.757, respectively. The average absolute deviation of the data from Equations (33) and (34) is 7.8 and 7.7%, respectively.

It is of interest to note that Equation (14) obtained by Reinhart for gaseous continuous phases (very low μ_c) is very similar to Equation (33) of this work.

Equations (31) through (34) are compared with the eccentricity data of typical systems in Figures 3, 4, and 5 for the following continuous phase viscosity regions: low viscosity (between 0.3 and 0.8 centipoise), moderate viscosity (between 0.8 and 2.5 centipoise), and high viscosity (between 2.5 and 46.0 centipoise). Examination of these figures and the calculated eccentricities of all other systems in the three viscosity regions indicates that those correlations with the Weber number are accurate over the entire range of μ_c studied. Those relations with just the Eötvös number [Equations (13), (33), and (34)] were reasonably accurate for the low and moderate viscosity regions but not for the high continuous phase viscosity region. It should be noted that the Eötvös number does not take into account μ_c (or μ_d), whereas the Weber number indirectly considers the effect of μ_c by means of the droplet velocity. It is suspected that additional data for high μ_c systems would result in an even greater overall average deviation of the observed eccentricities from those predicted by functions employing just the Eötvös number [Equations (13), (33), and (34)].

Equations (31) and (32) are recommended for the prediction of droplet eccentricity for the range of variables indicated in Tables 1 and 2. These equations require the calculation of the droplet velocity by one of the several existing droplet velocity correlations (*15, 17, 22*); however, in most design calculations the droplet velocity would be calculated in order to estimate such design parameters as mass transfer coefficients and contact time.

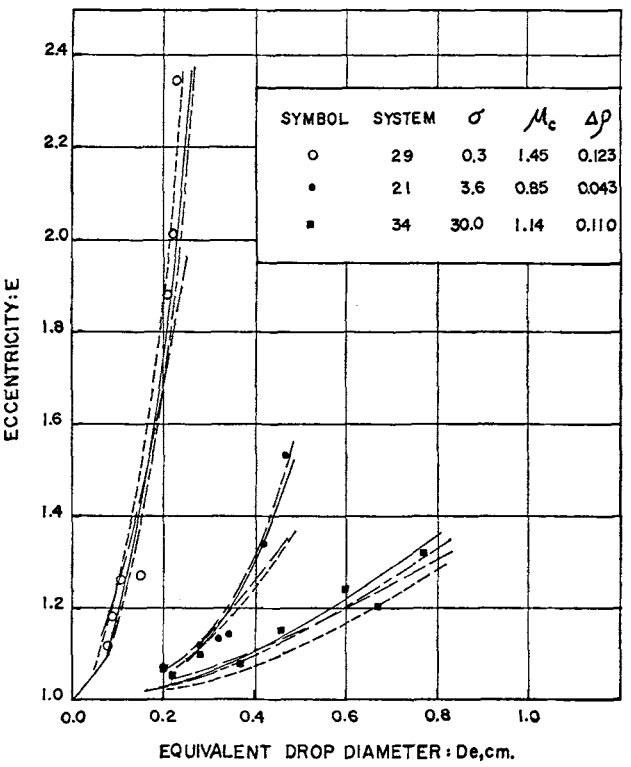

Fig. 4. Observed and calculated eccentricity as a function of drop diameter in the moderate μ_c region. Equation [31] — — —. Equation [32] ———. Equation [33] - - - - - - - - - - - -. Equation [34] — — —.

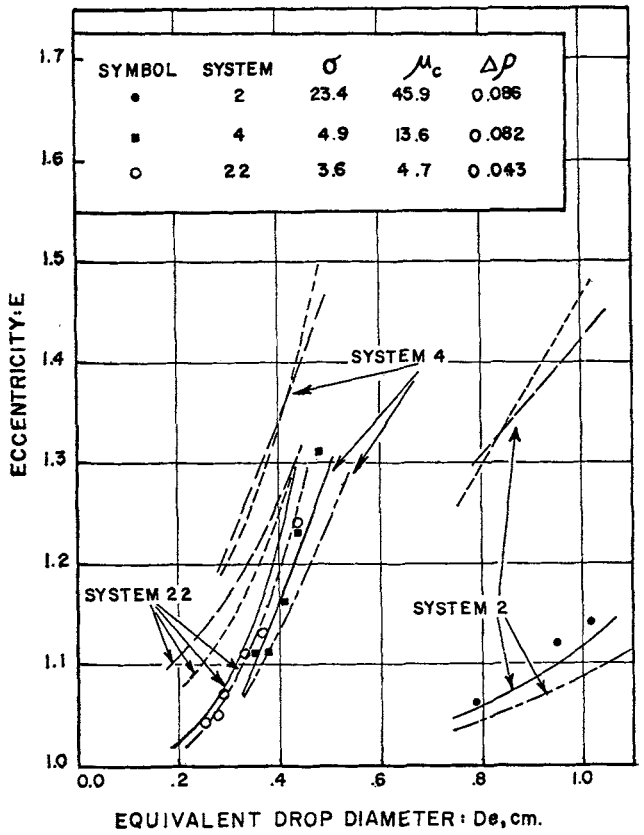

Fig. 5. Observed and calculated eccentricity as a function of drop diameter in the high μ_c region. Equation [31] — — — — —. Equation [32] ————. Equation [33] - - - - - - - - - - - - - - - - - -. Equation [34] — — — —.

Expansion of Equations (31) and (32) into the prirary variables indicates the relative effect of each primary variable on droplet eccentricity. However, since droplet velocity itself is a function of the various physical properties and drop size, the expansion of Equations (33) and (34) and the following direct least squares correlation of the primary variables* is somewhat more instructive:

$$E = 1 + 7.6\,\sigma^{-0.85}\,D_e^{1.97}\,\Delta\rho^{0.79}\,\mu_c^{-0.46}\,\mu_d^{-0.11} \quad (35)$$

The average absolute deviation of the data from Equation (35) is 8.0%. The confidence limits of the exponents at the 95% probability level are:

$$-0.85 \pm 0.11;\ 1.97 \pm 0.27;\ 0.79 \pm 0.14;\ -0.46 \pm 0.12;\ -0.11 \pm 0.06$$

The effect of interfacial tension essentially agrees with previous findings [see Equations (3) and (4)]. Droplet eccentricity is approximately proportional to $\Delta\rho^{0.8}$. The effect of equivalent diameter on the eccentricity of nonoscillating droplets is definitely *nonlinear*: $E \propto D_e^2$. If oscillating droplet data are included in the data analysis, the exponent of D_e is close to unity. An increase in the dispersed phase viscosity (which tends to reduce internal circulation) will cause a decrease in droplet eccentricity, all other variables held constant. The exponent m in Equation (5) was found to be approximately 0.10.

The effect of μ_c, never before reported, can be deduced from either Equations (32) or (35). From Equation (32), if all other variables are held constant (including droplet velocity), an increase in μ_c results in increased deformation. However, it is rather difficult to expect that an increase in μ_c would not affect the droplet velocity (*15, 17, 22*). Equation (35) indicates that, if all other physical properties and drop size are held constant, droplet deformation decreases if the continuous phase viscosity increases. This may also be deduced from Equation (32) if the approximate expression for the droplet terminal velocity of Klee and Treybal [Equation (5), reference 22] is substituted into the Weber number in Equation (32).

* Use cgs units and centipoise for viscosity.

SUMMARY

The eccentricity data of forty-five dispersed-continuous phase systems were analyzed in this investigation. Methods of predicting droplet shape previously reported in the literature and those developed in this work were compared with experimental data. The results and conclusions are summarized as follows:

1. The Hughes and Gilliland model of the droplet distortion process does not appear to be applicable to liquid-liquid systems. This was also reported earlier by Klee and Treybal.
2. Relatively simple relations involving the Eötvös number, Weber number, and viscosity ratio were obtained which enable the prediction of the eccentricity of nonoscillating droplets with average deviations of from 6 to 8% over a very wide range of Reynolds number. These correlations are more accurate than the Harmathy relation.
3. Eccentricity relations involving the Eötvös number do not appear to predict the effects of high continuous phase viscosities on droplet shape; the Weber number appears to be a more significant variable over all ranges of continuous phase viscosity encountered in this work.
4. The effect of density difference and interfacial tension on droplet eccentricity essentially agrees with previous findings. The eccentricity of nonoscillating droplets is approximately proportional to the second power of the equivalent drop diameter, not to the first power, as often reported. If all other physical properties and drop size are held constant, the effect of increasing both dispersed and continuous phase viscosities is to lessen the deformation of drops.
5. A relation for the eccentricity of a slightly deformed drop moving in streamline flow, obtained from the theoretical work of Taylor and Acrivos, was compared with experimental data. It predicts drop eccentricities quite accurately for Reynolds numbers less than about 20. A relation for eccentricity based on the theoretical development of Saito was less accurate than the previous relation based on the work of Taylor and Acrivos. Both relations are functions of the Weber number, viscosity ratio, and density ratio.
6. The relations developed in this work may be used with the theoretical expressions of Lochiel and Calderbank or the empirical expressions of Skelland and Cornish to estimate the resistance to mass transfer in the continuous phase flowing past oblate spheroidal particles.

ACKNOWLEDGMENT

The financial support of E. I. Du Pont De Nemours and Company in the form of a summer research grant to R. M. Wellek is gratefully acknowledged. A. H. P. Skelland received support from the National Science Foundation under grant number NSF GP-807. The Phillips Petroleum Company donated some of the solvents used in this work. The assistance of J. M. Patel with various computer calculations and of John Meek with part of the experimental work is also gratefully acknowledged.

NOTATION

a = equivalent droplet radius, $D_e/2$, cm.

$a_o, a_1, a_2, a_3, a_4, a_5$ = constants in Equation (30)

A_{os} = surface area of oblate spheroid, sq. cm.
A_s = surface area of a sphere, sq. cm.
b_o = constant in Equation (33)
b_1, b_2 = constants in Equation (34)
D = molecular diffusivity of solute in the continuous phase, sq. cm./sec.
D_e = equivalent droplet diameter, $[6V_d/\pi]^{1/3}$, cm.
D_H = horizontal diameter of droplet, $D_eE^{1/3}$, cm.
D_v = vertical diameter of droplet, $D_eE^{-2/3}$, $(D_{v,u} + D_{v,l})$, cm.
$D_{v,u}$ = upper semiminor axis of droplet, cm.
$D_{v,l}$ = lower semiminor axis of droplet, cm.
D_3 = characteristic dimension defined by Equation (16), cm.
e = parameter defined by Equation (18c)
E = droplet eccentricity, D_H/D_v
E_n = coefficients in the series expansion in Equation (21)
f_1, f_2 = functions
g = acceleration of gravity, cm./sec.^{2}
h = fineness ratio, $1/E$
j_D = j factor defined by Equation (15)
k = parameter defined by Equation (18b)
$(k_c)_s$, $(k_c)_{os}$ = individual continuous phase mass transfer coefficient for a sphere and oblate spheroid, respectively, g.-mole/(sec.) (sq. cm.) (g.-mole/cc.)
m = positive, but unknown, constant in Equation (5)
n = integer number in Equation (21)
N_{Eo} = Eötvös number, $(g\Delta\rho D_e^2/\sigma)$
N_{Fr} = Froude number, (U^2/gD_e)
N_{Re} = droplet Reynolds number, $(D_eU\rho_c/\mu_c)$
N'_{Re} = modified droplet Reynolds number, $(D_HU\rho_c/\mu_c)$
N''_{Re} = modified droplet Reynolds number, $(D_3U\rho_c/\mu_c)$
N_{Sc} = Schmidt number, (μ_c/ρ_cD)
N'_{Sh} = Sherwood number, $[(k_c)_{os}D_3/D]$
N_{Su} = surface tension group, $(\sigma D_e\rho_c)/(\mu_c^2)$, N_{Re}^2/N_{We}
N_{We} = Weber number, $D_eU^2\rho_c/\sigma$
$N\mu_r$ = viscosity ratio, μ_c/μ_d
$P_n(\cos\theta)$ = Legendre polynomial function of cos θ
$\mathbf{r}$ = position vector from center of spheroid to surface, cm.
R = $\mathbf{r}/a$
T = temperature, °C.
U = droplet velocity, cm./sec.
V_d = droplet or spheroid volume, cc.

Greek Letters

ρ_c, ρ_d = density of continuous and dispersed phase, respectively, g./cc.
$\Delta\rho$ = density difference, $|\rho_c - \rho_d|$, g./cc.
μ = cos θ
μ_c, μ_d = viscosity of continuous and dispersed phase, respectively, poise (unless stated otherwise)
$(\mu_a)_c$ = apparent viscosity of a non-Newtonian continuous phase at some specified shear rate, g.-m/(sec.)(cm.)
σ = interfacial tension, dynes/cm.
γ = distortion coefficient defined by Equation (8)
γ_1, γ_2 = functions defined by Equations (17) and (18a), respectively
Δ = functions defined by Equation (6) and (7)
θ = angle between vertical axis of spheroid and the position vector $\mathbf{r}$
$\psi(h)$ = $\psi(1/E)$ = function of h given in reference *16*
ψ_1 = function defined by Equation (20)
ψ_2, ψ_3 = functions defined by Equations (28) and (29), respectively
ζ, ζ_H, ζ_V = deformation of drop from a spherical shape (divided by a) as a function of μ, and in the horizontal and vertical directions, respectively
λ = function defined by Equation (23)

LITERATURE CITED

1. Baker, J. L. L., and B. T. Chao, *ME Tech. Rept. 1069-1*, Univ. Illinois, Urbana (1963).
2. Calderbank, P. H., and A. C. Lochiel, *Chem. Eng. Sci.*, **19**, 485 (1964).
3. Efroymson, M. A., "Mathematical Methods for Digital Computers," A. Ralston and H. S. Wilf, ed., p. 191, Wiley, New York (1964).
4. Elzinga, E. R., Jr., and J. T. Banchero, *A.I.Ch.E. J.*, **7**, 394 (1961).
5. Fararoui, A., and R. C. Kintner, *Trans. Soc. Rheol.*, **5**, 369 (1961).
6. Farmer, W. S., *ORNL 635* (1950).
7. Garner, F. H., and P. J. Haycock, *Proc. Roy. Soc.*, **A252**, 457 (1959).
8. Garner, F. H., K. D. Mathur, and V. G. Jenson, *Nature*, **180**, 331 (1957).
9. Garner, F. H., and A. H. P. Skelland, *Chem. Eng. Sci.*, **4**, 149 (1955).
10. Garner, F. H., and M. Tayeban, *Anal. Real Soc. Espan. Fis. Quim. (Madrid)*, **B56**, 479 (1960).
11. Griffith, R. M., *Chem. Eng. Sci.*, **12**, 198 (1960).
12. Hamielec, A. E., and A. I. Johnson, *Can. J. Chem. Eng.*, **40**, 41 (1962).
13. Harmathy, T. Z., *A.I.Ch.E. J.*, **6**, 281 (1960).
14. Heertjes, P. M., W. A. Holve, and H. Talsma, *Chem. Eng. Sci.*, **3**, 122 (1954).
15. Hu, S., and R. C. Kintner, *A.I.Ch.E. J.*, **1**, 42 (1955).
16. Hughes, R. R., and E. R. Gilliland, *Chem. Eng. Progr.*, **48**, 497 (1952).
17. Johnson, A. I., and L. Braida, *Can. J. Chem. Eng.*, **35**, 165 (1957).
18. Johnson, A. I., and A. E. Hamielec, *A.I.Ch.E. J.*, **6**, 145 (1960).
19. Keith, F. W., and A. N. Hixson, *Ind. Eng.*, **47**, 258 (1955).
20. Kintner, R. C., "Advances in Chemical Engineering," T. B. Drew, J. W. Hoopes, and Theodore Vermeulen, ed., Vol. 4, p. 51, Academic Press, New York (1963).
21. ———, T. J. Horton, R. E. Graumann, and S. Amberkar, *Can. J. Chem. Eng.*, **39**, 235 (1961).
22. Klee, A. J., and R. E. Treybal, *A.I.Ch.E. J.*, **2**, 444 (1956).
23. Linton, M., and K. L. Sutherland, *Chem. Eng. Sci.*, **12**, 214 (1960).
24. Lochiel, A. C., and P. H. Calderbank, *ibid.*, **19**, 471 (1964).
25. Mhatre, M. V., and R. C. Kintner, *Ind. Eng. Chem.*, **51**, 865 (1959).
26. Olney, R. B., and R. S. Miller, "Modern Chemical Engineering," A. Acrivos, ed., Vol. 1, p. 89, Reinhold, New York (1963).
27. Pasternak, I. S., and W. H. Gauvin, *Can. J. Chem. Eng.*, **38**, 35 (1960).
28. Reinhart, A., *Chem. Ing. Tech.*, **36**, 740 (1964).
29. Riabouchinsky, D. P., *Aerodyn. Inst. Koutchino*, **5**, 73 (1921); translated in *Natl. Advisory Comm. Aeronaut. Tech. Note No. 44.*
30. Rybczynski, W., *Bull. Acad. Sci. Cracow (A)*, 40 (1911).
31. Saito, S., *Sci. Rept. Tohoku Imp. Univ.*, **2**, 179 (1913).
32. Skelland, A. H. P., and A. R. H. Cornish, *A.I.Ch.E. J.*, **9**, 73 (1963).
33. Skelland, A. H. P., and R. M. Wellek, *ibid.*, **10**, 491 (1964).
34. Spilhaus, A. F., *J. Meteor.*, **5**, 108 (1948).
35. Taylor, T. D., and A. Acrivos, *J. Fluid Mech.*, **18**, 466 (1964).
36. Treybal, R. G., "Liquid Extraction," Vol. 2, p. 186, McGraw-Hill, New York (1963).
37. Warshay, M., E. Bogusz, M. Johnson, and R. C. Kintner, *Can. J. Chem. Eng.*, **37**, 29 (1959).
38. Wellek, R. M., and A. H. P. Skelland, *A.I.Ch.E. J.*, **11**, 557 (1965).
39. Garner, F. H., and D. A. Lihou, *Dechema Monographs*, **55**, (955-975) 155-178 (1965).

Manuscript received September 9, 1965; revision received December 20, 1965; paper accepted January 12, 1966. Paper presented at A.I.Ch.E. Atlantic City meeting.